EOF and SVD Analysis of SST and SLP in the Persian Gulf

S. Hassanzadeh*, A. Kiasatpour and F. Hosseinibalam
Physics Department University of Isfahan, Isfahan ٨١٧٤٦ Iran
Keywords: Singular Value Decomposition, Atmospheric Pressure, Persian Gulf, Lag

Abstract:

The atmosphere and the underlying ocean are closely coupled. The ocean plays an important role in establishing and changing the earth's climate. Both the ocean and the atmosphere transport energy and exchange it with each other and their dynamics are coupled through exchange processes at their common interface.
The main goal of this paper is to investigate the air-sea interactions on interannual and decadal time scale in the Persian Gulf.
٣٤ years of data (١٩٦٧-٢٠٠) are used to investigate air-sea interaction in the Persian Gulf. An Empirical Orthogonal Function (EOF) and Singular Value Decomposition (SVD) analysis are applied to determine the coupled modes of variability of monthly Sea Surface Temperature (SST) and Sea Level Pressure (SLP). We find that the

The four leading EOF patterns of SST are found. These modes together account for ٩٩,٨٪ of the total monthly SST variance. Individually they explain ٩٠,٩٪, ٧,٥٪, ١٪ and ٠,٤٪ of the variance. According to the North el al. (١٩٨٢), the difference between the forth and fifth eigenvalue is comparable to the magnitude of the sampling errors, which means that the error in the EOFs is comparable to the size of the EOFs themselves. The temporal variability of each EOF, obtained by the expansion coefficient of spatial patterns .
EOF١ exhibits a generally southeast-northwest gradient over the entire region. This mode accounts for up to ٩٠,٩٪ of the variance. This is due to the principal features of the long time Persian Gulf circulation driven by the Oman Sea waters through the strait of Hormuz along the Iranian coasts. This cyclonic gyre before turning around the central Gulf basin forms a second cyclonic gyre. The front which separate these gyres is denoted by the zero contour in the EOF١ isotherms.
EOF٢ displays a monopole pattern locating in the central basin of the Gulf and extending over the middle portion of the Gulf. By and large, the second EOF resembles west and east of this monopole a copy of the meridional isotherm pattern of the first EOF.
The third EOF is mainly associated with north-south gradient and isotherms extend zonally. This mode explains ١٪ of the variance. The forth EOF shows a dipole like structure with one pole centered around the front separated the gyres. This mode account for ٠,٤٪ of the variance and it is not significant.
The time series of EOFs are obtained and characterized by a different time variability. The four spatial patterns of EOFs for SP fields which account for ٩٤,٣٦٪ of the total variance are calculated as well.
EOF١ has northeastward gradient, which is in the direction of Shomal wind (northwesterly). This mode account for ٥٣,٠٪ of the variance. The second EOF of SLP has a structure which is related to west-east changes in the direction of the pressure

gradient. A monopole structure can be seen in the EOF[٣] centered in the north head of the Gulf.

* Corresponding author. Tel: +٩٨ ٣١١ ٧٩٣٢٤٢٣ Fax: +٩٨ ٣١١ ٧٩٣٢٤٠٩.
E-mail address: shz@sci.ui.ac.ir

١-Methods:

١-١ EOF

We have used the method of the principal component analysis, often referred to as empirical orthogonal function (EOF) analysis. This method partitions the temporal variance of the highly correlated data into a small number of orthogonal spatial patterns called eigenvectors and corresponding orthogonal time coefficients. The input data matrix X is of dimension N x n over N time steps on n grid points , with i indexing time (cases) and j indexing grid points (variables). The value of the field at any point in time and space is then denoted X_{ij}. A new set of variables Z are formed as linear combinations of the original variables, weighted by the coefficients E.

$$Z_{ij} = \sum_{m=1}^{r} x_{im} e_{mj} \quad i = 1,...,N; j = 1,...,n, r =\leq n \qquad (١)$$

or, in matrix notation:

$$Z = XE \qquad (٢)$$

The E matrix contains what will be subsequently referred to as the eigenvectors (or EOFs) and the Z matrix the PCs (Temporal). In this arrangement, a single column of Z is one PC and a single row of E is its associated EOF. When rearranged as (٣), we see that the original dataset can be reconstructed from the PCs and EOFs.

$$X = ZE^T \qquad (٣)$$

The EOFs are uncorrelated with each other, hence the EOF matrix multiplied by its transpose yields the identity matrix:

$$EE^T = I \qquad (٤)$$

The variance/covariance matrix for the original (C) and transformed (Λ) datasets are given respectively by (٥) and (٦):

$$C = \frac{1}{(N-1)} X^T X \qquad (٥)$$

$$\Lambda = \frac{1}{(N-1)}(XE)^T(XE) = \frac{1}{(N-1)}(Z)^T(Z) \qquad (٦)$$

The following relationships then exist between C and Λ:

$$C = E\Lambda E^T \qquad (٧)$$

$$CE = \Lambda E = (\lambda)E \qquad (٨)$$

The last term in (٨) derives from the fact that the off-diagonal elements of Λ are zero due to the orthogonality of the PCs. The solution to maximizing (٢), i.e., the variance of successive PCs, subject to the condition (٤) requires solving the matrix equation:

$[C - \lambda I]E = ٠$ (٩)

That is, one must find the characteristic roots (eigenvalues (λ)) and eigenvectors of the data covariance matrix.

١-٢ SVD

Singular value decomposition (SVD) is the multivariate statistical technique used in the atmospheric and marine sciences. It is usually applied to two combined fields such as SST and SLP.

Let X denote an m ×n matrix of real-valued data and rank r. The equation for singular value decomposition of X is the following:

$$X = USV^T \qquad (١٠)$$

Where U is an m×n matrix, S is an n×n diagonal matrix, and V ^{T} is also an n×n matrix. The elements of S are only nonzero on the diagonal, and are called the singular values. Thus, S = diag($S_١$,...,S_n). Furthermore, $S_k > ٠$ for $١ \le k \le r$, and $S_i = ٠$ for $(r+١) \le k \le n$. Note that for a square, symmetric matrix X, singular value decomposition is equivalent to diagonalization, or solution of the eigenvalue problem.

$$X^{(l)} = \sum_{k=1}^{l} U_k S_k V_k^T \qquad (١١)$$

is the closest rank-l matrix to X. The term "closest" means that $X(l)$ minimizes the sum of the squares of the difference of the elements of X and $X(l)$, $\sum ij\,|X_{ij} - X(l)_{ij}|^٢$. One way to calculate the SVD is to first calculate V^T and S by diagonalizing $X^T X X$:

$$X^T X = VS^2V^T \qquad (١٢)$$

and then to calculate U as follows:

$$U = XVS^{-1} \qquad (١٣)$$

V or U may be calculated using the Gram-Schmidt orthogonalization process.

٣- The Variability of SST and SLP: EOF Analysis

We start with a description of the independent variability of the sea surface temperature and atmospheric sea level pressure during the ٣٤ y period using EOF analyses. **٣-١ EOF analysis of SST**

The four leading EOF patterns of SST are shown in Figure ١. These modes together account for ٩٩,٨٪ of the total monthly SST variance. Individually they explain ٩٠,٩٪, ٧,٥٪, ١,٠% and ٠,٤٪ of the variance. The temporal variability of each EOF, which obtained by the expansion coefficient of spatial patterns are depicted in Figure ٢.

EOF١ (Figure ١) exhibits a generally southeast-northwest gradient over the entire region. This mode accounts for up to ٩٠,٩٪ of the variance. This is due to the principal features of the long time Persian Gulf circulation driven by the Oman Sea waters through the strait of Hormuz along the Iranian coasts. This cyclonic gyre before turning around the central Gulf basin forms a second cyclonic gyre. The front which separate these gyres is denoted by the zero contour in the EOF١ isotherms.

EOF٢ (Figure ١) displays a monopole pattern locating in the central basin of the Gulf and extending over the middle portion of the Gulf. By and large, the second EOF resembles west and east of this monopole a copy of the meridional isotherm pattern of the first EOF. The third EOF is mainly associated with north-south gradient and isotherms extend zonally. This mode explains ١٪ of the variance. The forth EOF shows a dipole like structure with one pole centered around the front separated the gyres. This mode account for ٠,٤٪ of the variance and it is not significant.

The time series of EOFs for SST are shown in Figure ٢ and characterized by an interannual fluctuations.

٣-٢ EOF Analysis of SLP

Figure ٣ shows the four spatial patterns of EOFs for SLP fields which account for ٩٤,٤% of the total monthly SLP variance.

EOF١ (Figure ٣) has northsouthward gradient, which is in the direction of Shamal wind (northwesterly). This mode account for ٥٣,٠٪ of the variance. The second EOF of SLP (Figure ٣b) has a structure which is related to west-east changes in the direction of the pressure gradient. A monopole structure can be seen in the EOF٣ (Figure ٣c) centered in the north head of the Gulf.

The time series of EOFs for SLP are shown in Figure ٤. A frequency analysis of the corresponding time series reveals an oscillatory behavior of the fields.

Spectral analysis of the temporal amplitude was done for all SST and SLP modes. All EOFs of the SLP show a dominant frequency associated with a ten month period, but the SST modes reveal a twelve month period. Figure ٥ shows the spectra of both the first EOF of the SLP (dashed line) and SST(tick line). Spectral analysis of SST indicates several small peaks at month periods as well. Atmospheric pressure leads the sea surface temperature by two months suggesting an air-to-sea driving.

٣-٣ Relating Marine and Atmospheric behaviors

To look for possible air-sea interaction, the correlation coefficients between the time series of the four discussed SST and SLP modes are calculated (are not shown). The

time series EOF١ (SLP) and EOF٢ (SST) are significantly negatively correlated. The series EOF٢ (SLP) and EOF١ (SST) are also significantly correlated. Lagged cross correlations between the two modes exhibit three significant correlations. One of these shows the air leading the sea by ١ months suggesting again the presence of an atmosphere-to-sea forcing. The others (at -٦ and -١١ months) are probably a reflection of the ½ year and about one year periodicity that exist in the two time series. That is, two time series are out of phase at a lag equal to half the period of oscillation about ٦ and ١١ months.

٤-SVD Analysis

The two leading SVD modes of the coupled SST and SLP variations account for ٩٩,٩٪ of the total square variance. Each mode independently accounts ٩٦,٦٪ and ٣,٣٪ of the total square covariance respectively. The correlation coefficients between the first two modes of SST and SLP are calculated as well. The correlation between SVD١(SLP) and SVD١(SST) is ٠,٩٦, and the correlation between SVD٢(SLP) and SVD٢(SST) is ٠,٩٤. Thus, the SVD modes provide more information on the coupling between the fields than the modes obtained by EOF methods.

Lagged correlation analysis between SVD١(SLP) and SVD١(SST) indicates that the coupling is strongest when SLP leads SST by -١٢, -٦, ٦ and ١٢ months. Therefore the first mode of the SVD analysis seems depict an air-to-sea forcing, in which the sea response to the atmospheric changes appears with an semiannual and interannual time lag. The first mode exhibits a strong and highly significant coupling between SST and SLP. Figure ٦ depicts the spatial patterns and the expansion coefficient of the first SVD mode of the coupled fields. The SST mode pattern closely resemble those obtained for the first EOF and SVD (figures ٦a and ١). On the other hand, the SLP pattern for the first SVD mode dose not resemble the SLP modes. Figure ٧ shows the components of the second SVD mode of coupled fields. The SLP time series for the first EOF mode resemble those of the second SVD mode of the SLP, but the spatial pattern of SLP for the second EOF mode closely resemble those of the second SVD mode, with the signs reversed. The SST spatial pattern of the second mode closely resemble those of obtained by EOF and SVD. There is also some similarity between the SST times series of the second SVD mode and those of the first EOF mode.

٥-Summary:

The principal features that characterize the individual modes of SST and SLP behavior are found again in the SVD of the coupled fields. The two leading SVD modes of variability of the coupled SST and SLP fields have been identified and analyzed. The leading modes account for ٩٩,٦٪ of the total variance. The main patterns of both variables of variability of both variables independently provide considerable information on the coupling, but only one of the two variables dominates each of the two first coupled modes. While the first coupled mode keeps the characteristics of the main SLP (independent) pattern, the second coupled mode repeats the behavior of the main SST (independent) mode, suggesting the relative importance of each component of the system in each discussed coupled mode.

The first coupled mode of variability between the sea surface temperature and atmospheric pressure can be described as a strengthening and weakening of the cyclonic

gyres, which seems to force fluctuations in a north-south dipole structure in the sea surface temperature by Ekman upwelling which is wind related processes. The atmospheric forcing of the SST changes is detectable in the sea with a lag of ١ and ٦ months. The observed fluctuations are dominated by an interannaul timescales (١٢ months).

Acknowledgments:

The authors wish to thank the office of Graduate Studies of the University of Isfahan for their support.

References:

١-Berreta, A., H. E. Roman, F. Raicich and F. Crisciani, (٢٠٠٤) Long-time correlations of sea level and atmosphere pressure fluctuations at Trieste, Physica A, ٣٤٧(٢٠٠٤)٦٩٥-٧٠٣.

٢-Mann, M. E. and J. Park, Global-scale modes of surface temperature variability on interannual to century time scale, J. Geophys. Res. ٩٩, ٢٥٨١٩-٢٥٨٣٣, ١٩٩٤.

٣-Deser, C., and M. L. Balckman, Surface climate variations over the North Atlantic Ocean during winter, J. Climate ١٠, ٣, ٣٩٣-٤٠٨, ١٩٩٣.

٤-Hassanzadeh, S., ١٩٩٧. Interannual Variability in the Ocean and Atmosphere in the ١٩٨٠s and early ١٩٩٠. Ph.D. Thesis, pp. ١٧٥.

٥٥-Venegas, S. A., L. A. Mysak and D. N. Straub, Evidence for interannual and interdecadal climate variability in the South Atlantic, Geophys. Res. Lett., ٢٣, ٢٦٧٣-٢٦٧٦, ١٩٩٦.

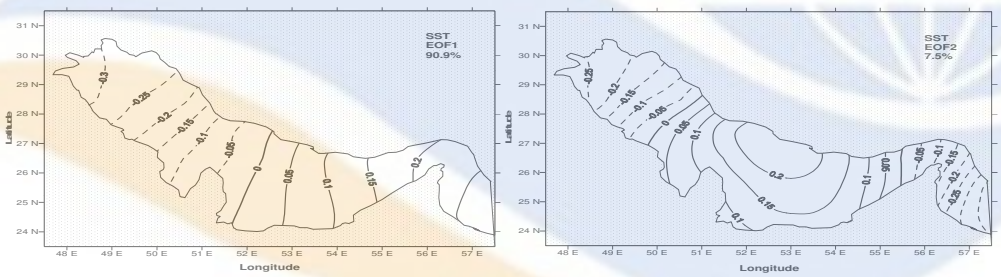

Figure:١ Spatial patterns of the four EOF modes of SST. Negative contours are dashed. Zero line is ticker.

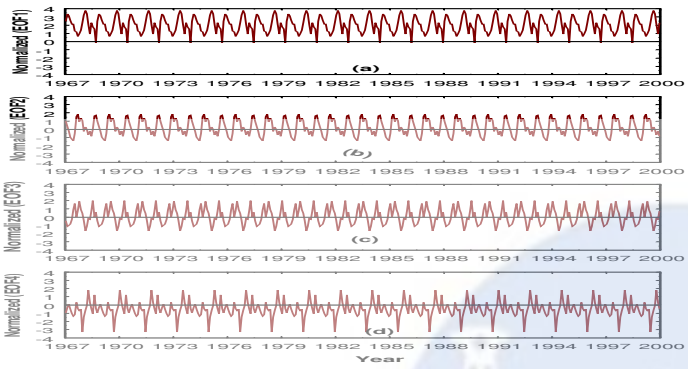

Figure:۲ Time series of expansion coefficients of the four EOF modes of SST. The time series are normalized by the standard deviation.

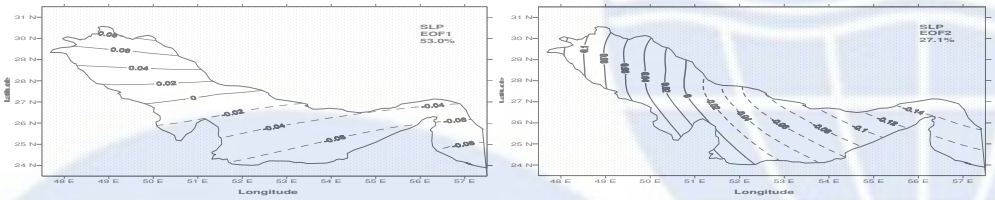

Figure:۳ Spatial patterns of the four EOF modes of SLP. Negative contours are dashed. Zero line is ticker.

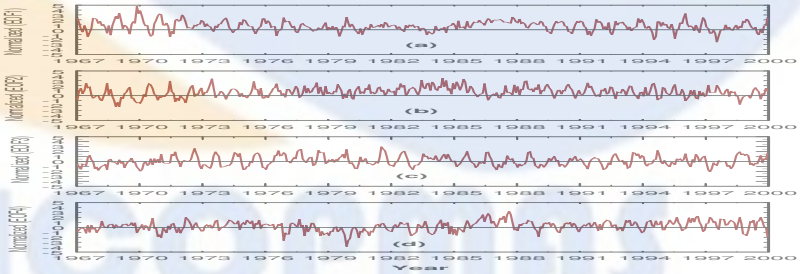

Figure:٤ Spatial patterns of the four EOF modes of SLP. Negative contours are dashed. Zero line is ticker.

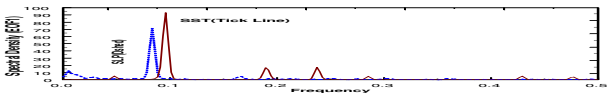

Figure: ٥ Spectra of the first EOF time series of the SST (solid) and SLP (dashed).

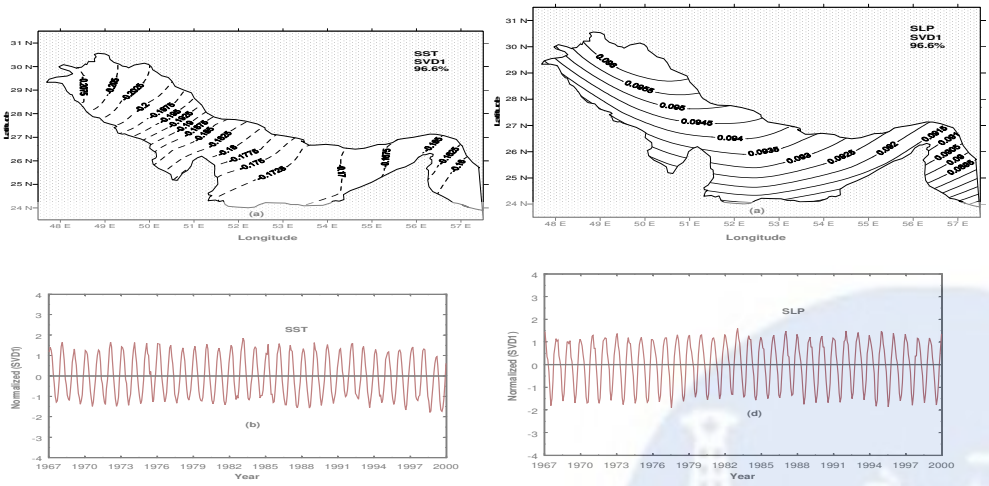

Figure:٦ Spatial and expansion coefficient of the first SVD coupled mode of SST and SLP.

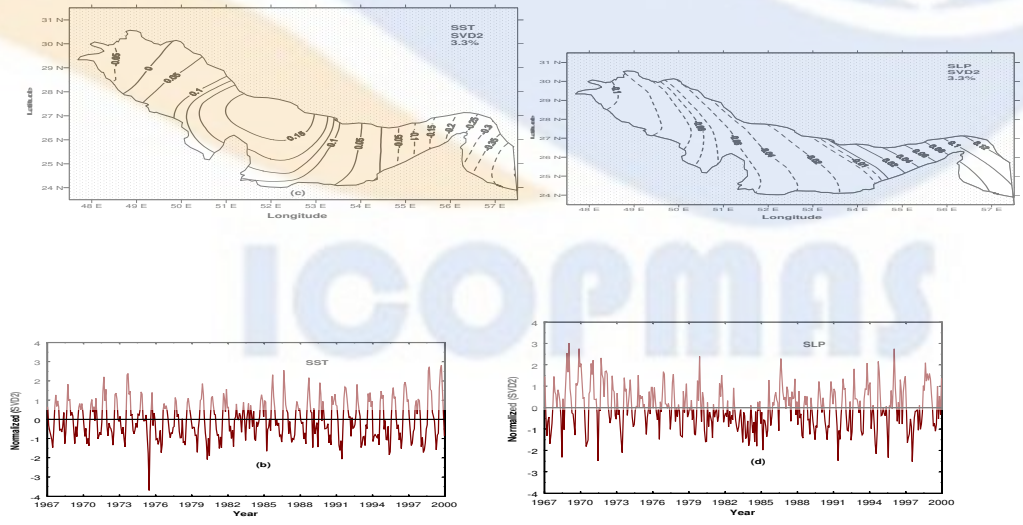

Figure:٧ Spatial and expansion coefficient of the second SVD coupled mode of SST and SLP. Negative contours are negative and zero line is ticker. The time amplitudes are normalized by the standard deviation.

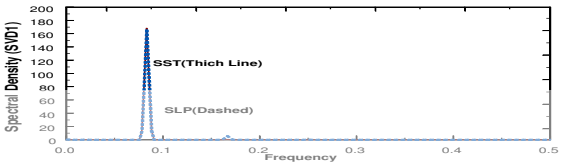

Figure:۸ Spectra of the first SVD time series for the SST (solid) and SLP (dashed).